

ALP-portal majorana dark matter

Shivam Gola,^{1,2,*} Sanjoy Mandal,^{3,†} and Nita Sinha^{1,2,‡}

¹*The Institute of Mathematical Sciences,*

C.I.T Campus, Taramani, Chennai 600 113, India

²*Homi Bhabha National Institute, BARC Training School*

Complex, Anushakti Nagar, Mumbai 400094, India

³*AHEP Group, Institut de Física Corpuscular,*

CSIC/Universitat de València, Parc Científic de Paterna.

C/ Catedrático José Beltrán, 2 E-46980 Paterna (Valencia), Spain

Axion like particles(ALPs) and right handed neutrinos (RHNs) are two well-motivated dark matter(DM) candidates. However, these two particles have a completely different origin. Axion was proposed to solve the Strong CP problem, whereas RHNs were introduced to explain light neutrino masses through seesaw mechanisms. We study the case of ALP portal RHN DM (Majorana DM) taking into account existing constraints on ALPs. We consider the leading effective operators mediating interactions between the ALP and SM particles and three RHNs to generate light neutrino masses through type-I seesaw. Further, ALP-RHN neutrino coupling is introduced to generalize the model which is restricted by the relic density and indirect detection constraint.

Keywords: Axion like particle, Heavy Neutrinos, Dark matter

1. INTRODUCTION

Dark matter is one of the most important issues of modern particle physics and cosmology. Although a wide variety of experiments ranging from sub-galactic scale to a large cluster of galaxies have accumulated data in support of DM's existence [1–5], its microscopic properties still remain unknown. Several DM candidates have been proposed and searched for, however, no completely satisfactory DM candidate has been found so far. Among a lot of possibilities, the axion and sterile neutrinos can be regarded as a leading candidates for DM. These particles arise in well-motivated extensions of the Standard Model and have very rich phenomenology.

* shivamg@imsc.res.in

† smandal@ific.uv.es

‡ nita@imsc.res.in

It is known from the cosmological observations that the sum of the active neutrino masses $\sum m_\nu \leq 0.12$ eV [6, 7] and contribution to the relic density $\leq 4.5 \times 10^{-3}$, which is too low to explain the DM abundances today, hence there is no explanation for DM within the SM. However, a new heavier neutrino field could explain DM and it is naturally required to explain the masses of active neutrinos as inferred from the oscillation experiments [8]. The discovery of neutrino oscillations confirming the existence of at least two non-vanishing neutrino mass-squared differences necessitate physics beyond the Standard Model (BSM). In principle neutrino mass could be simply generated by addition of right-handed neutrinos (RHNs) to the SM particle content. These RHNs interact with SM fields via mixing with active neutrinos. Since RHNs are SM singlet, they allow Majorana mass term along with usual Dirac mass term. This is known as type-I seesaw mechanism [9–12]. Mass of these RHNs could range from eV to GUT scale depending on the models [13–16]. RHNs can also play the role of warm dark matter (WDM), which is singlet under the SM gauge symmetry and has tiny mixing with the SM neutrinos leading to a long lifetime [17–19]. Also, KeV scale RHNs have been studied as a viable DM candidate [20–22]. In this work we have instead focused on the prospects of having GeV scale RHNs as a Weakly interacting massive particle (WIMP) DM candidate.

Axion [23] was postulated in the Peccei-Quinn (PQ) mechanism to solve the strong CP problem [24–27] of quantum chromodynamics (QCD). This axion can be identified as a (pseudo) Nambu-Goldstone boson associated with the spontaneous breaking of the $U(1)_{\text{PQ}}$ global symmetry [28–30]. This QCD axion gets a tiny mass from the explicit breaking of this global symmetry due to QCD anomaly. Astrophysical and experimental searches have not favoured the PQ model. To resolve issues with PQ model, other popular solutions like KSVZ [31, 32], DFSZ [33] etc. invoking axion were also proposed and studied afterwards. The magnitude of the couplings of axions to ordinary matter is inversely proportional to the axion decay constant f_a which is associated with the $U(1)_{\text{PQ}}$ symmetry breaking scale. Hence, the couplings are highly suppressed if f_a is sufficiently large and this features make the axion suitable to be a DM candidate. Many BSM extensions which features spontaneously broken global $U(1)$ symmetry predict massless Nambu-Goldstone bosons whose couplings are not constrained unlike the original QCD axion. These kind of particles are known as axion like particles (ALPs). Mass of these ALPs are not related to its symmetry breaking scale unlike PQ axion. In general they are not supposed to solve the strong CP problem, but with the introduction of planck scale operators they could solve the strong CP problem [34, 35]. Here we will consider the most general $SU(2)_L \otimes U(1)_Y$ invariant formulation of ALP interactions developed in Refs. [36–38]. This generic effective ALPs Lagrangian allows ALPs coupling with all the SM gauge bosons as well as with all the SM fermions. In addition to this effective ALP Lagrangian, we introduce three RHNs which can generate light neutrino masses through type-I seesaw. We invoke a \mathbb{Z}_2 symmetry under

	Standard Model						New Fermions		New Scalar
	ℓ_L	e_R	q_L	u_R	d_R	H	N_1	$N_{2,3}$	a
$SU(2)_L$	2	1	2	1	1	2	1	1	1
$U(1)_Y$	-1/2	-1	1/6	2/3	-1/3	1/2	0	0	0
\mathbb{Z}_2	+	+	+	+	+	+	-	+	+

TABLE I: Matter content and charge assignment of the considered model.

which all SM and BSM particles are even except the lightest RHN. Further we introduced the RHN-ALP coupling and show that the lightest RHN (Singlet majorana fermion) which is odd under \mathbb{Z}_2 can play the role of DM candidate. Note that the phenomenology of this ALP-mediated DM [39] will be similar to pseudoscalar-portal DM. Also DM interacting via the exchange of a light ALP can induce observable signals in indirect detection experiments while evading the strong bounds from direct DM searches. Note that ALPs with mass $M_a \sim \mathcal{O}(\text{GeV})$ may also show up at colliders [40–42] or in rare meson decays [43–45].

Rest of the manuscript is organized as follows. In Sec. 2 we introduced our model, detailing the new interactions present. In Sec. 3 we summaries the existing constraints on ALP parameter space coming from various observables and collider searches. In Sec. 4 we have explored and discussed the feasible parameter space coming from DM analyses such as relic density, direct and indirect detection. Finally, we give our conclusions in Sec. 5.

2. MODEL

The model that we consider is the minimal combination of type-I seesaw and effective ALP interaction with additional \mathbb{Z}_2 symmetry apart from the SM gauge symmetry [46, 47]. The matter content of the model is shown in Table. I. Let’s first briefly discuss the features of a generic ALP Lagrangian. We extend the SM particle content by adding an additional ALP which is a singlet under SM charges and is a pseudo Nambu-Goldstone boson of a spontaneously broken symmetry at some energy which is higher than the electroweak scale v . In effective theory the operators will be weighted by powers of a/f_a , where f_a is the scale associated to the physics of the ALP, a . Effective linear Lagrangian with one ALP has been already discussed in great detail in Ref. [36, 37]. For linear EWSB realizations the most general linear bosonic Lagrangian involving a is given by,

$$\mathcal{L} = \mathcal{L}_{\text{SM}} + \mathcal{L}_{\text{ALP}}, \quad (1)$$

where the leading order effective Lagrangian \mathcal{L}_{SM} is same as the SM one and with

$$\begin{aligned} \mathcal{L}_{\text{ALP}} = & \frac{1}{2}\partial_\mu a \partial^\mu a - \frac{1}{2}M_a^2 a^2 - \frac{C_{\tilde{G}}}{f_a} a G_{\alpha\mu\nu} \tilde{G}^{\mu\nu\alpha} - \frac{C_{\tilde{B}}}{f_a} a B_{\mu\nu} \tilde{B}^{\mu\nu} - \frac{C_{\tilde{W}}}{f_a} a W_{\alpha\mu\nu} \tilde{W}^{\alpha\mu\nu} \\ & + iC_{a\Phi} \times [(\bar{Q}_L Y_U \tilde{\Phi} u_R - \bar{Q}_L Y_D \Phi d_R - \bar{L}_L Y_E \Phi e_R) \frac{a}{f_a} + h.c.] \end{aligned} \quad (2)$$

Here Φ and a are the Higgs and ALP fields respectively. C_i where $i = G, B, W, a\Phi$ are the corresponding Wilson coefficients for ALP-gauge boson and ALP-matter interactions. Parameters M_a and f_a are the ALP mass and energy scale associated to ALP physics. Y_D , Y_U and Y_E are 3×3 matrices in flavour space which stands for down-type quarks, up-type quarks and charged leptons, respectively. We see that ALP Lagrangian has a very generic form than that of the QCD-axion, where the mass of ALP is not restricted by the new physics scale. The remaining fields and parameters are the same as in SM. References [37, 48, 49] have discussed the phenomenology of the various pieces of the model. Now let's introduce the type-I seesaw Lagrangian with three additional SM singlet RHNs:

$$\mathcal{L}_{\text{RHN}} = i \sum_{i=1}^3 \bar{N}_i \gamma^\mu \partial_\mu N_i - \sum_{j=2}^3 Y_{\alpha j} \bar{L}_\alpha \tilde{\Phi} N_j - \sum_{i,j=2}^3 M_{ij} \bar{N}_i^c N_j - M_{N_1} \bar{N}_1^c N_1 + \text{h.c.} \quad (3)$$

where N_i are the SM singlet RHNs, $Y_{\alpha j}$ is the Dirac Yukawa coupling and M_{ij} is the Majorana mass term. As, N_1 is odd under \mathbb{Z}_2 symmetry, Dirac type of Yukawa interaction is forbidden for it unlike that for $N_{2,3}$. As a result of this, one of the light neutrinos will remain massless and we have enough parameters to describe the neutrino oscillations data. In addition to this, \mathbb{Z}_2 symmetry stabilizes the N_1 and it can play the role of DM candidate if one allows the following ALP-RHN interaction,

$$\mathcal{L}_{\text{ALP-RHN}} = - \sum_{i=1}^3 \frac{C_{aN_i}}{f_a} (\bar{N}_i \gamma^\mu \gamma^5 N_i) \partial_\mu a, \quad (4)$$

where C_{aN_i} denotes the ALP-RHNs Wilson coefficient and through this DM particle N_1 can communicate with the ALP sector. We call this ALP-portal RHN DM. We consider ALP mass of the order of few hundreds of MeV to GeV. We have considered N_1 to have mass up to few TeV. In the next section we discuss the allowed range for the several parameters of the model from the various phenomenological bounds.

3. EXISTING CONSTRAINTS ON ALP PARAMETER SPACE

Before diving into the details of DM analyses, let's first recall the existing experimental bounds on the couplings of ALPs to gluons, photons, fermions and also from collider searches with $f_a \sim \mathcal{O}(1 \text{ TeV})$ [40, 41, 43, 44, 50–61]. ALP photon coupling is the primary parameter

through which astrophysical and cosmological bounds are set on such particles. The ALP and photon coupling can be deduced

$$\mathcal{L}_{a\gamma} = -C_{a\gamma} a F_{\mu\nu} \tilde{F}^{\mu\nu}, \text{ with } C_{a\gamma} = \frac{(C_{\tilde{B}} \cos^2 \theta_w + C_{\tilde{W}} \sin^2 \theta_w)}{f_a} \quad (5)$$

Particularly experiments like CAST, using primakoff process, constrained the parameter space ($M_a - C_{a\gamma}$) heavily for M_a smaller than few eV [62]. For $M_a \sim 1$ MeV the best present constraint comes from Beam Dump experiments, $C_{a\gamma}/f_a \leq 10^{-5} \text{ GeV}^{-1}$ [40]¹. A slightly higher mass range is constrained by the collider experiments such as LEP and LHC [40]. In LEP, the process like $e^-e^+ \rightarrow \gamma a \rightarrow 3\gamma$ is being analysed to constrain the coupling whereas in LHC it is $pp \rightarrow \gamma a$ which searched for mono, di or tri photon signals. All these constraints are described in the references [37, 63, 64]. A limite on axion gauge boson coupling $C_{\tilde{W}}/f_a < 10^{-5} \text{ GeV}^{-1}$ is obtained for $0.175 \leq M_a \leq 4.78 \text{ GeV}$ by analysing of the process $B^\pm \rightarrow K^\pm a, a \rightarrow \gamma\gamma$ at the BABAR experiment [65]. Constraint on $C_{\tilde{G}}$ is set by mono jet 8 TeV LHC analysis. Unlike $C_{a\gamma}$, here it is much more complicated to put bound on $C_{\tilde{G}}$ due to large numbers of diagrams involved in the process. However, the dominant digram was found to be $gg \rightarrow ag$, which is complicated due to hadronisation that leads to jets in the final state. These constraints have been analysed in the reference [40, 55]. The limit from this study reads as $C_{\tilde{G}}/f_a \leq 10^{-4} \text{ GeV}^{-1}$ for $M_a \leq 0.1 \text{ GeV}$. Also the bound on $\text{BR}(K^+ \rightarrow \pi^+ + \text{nothing})$ [66] can be used to constrain the process $K^+ \rightarrow \pi^+ + \pi^0 (\pi^0 \rightarrow a)$ which can be reinterpreted in terms of ALP-gluon coupling $C_{\tilde{G}}$, yielding $C_{\tilde{G}}/f_a \leq 10^{-5} \text{ GeV}^{-1}$ for $M_a \leq 60 \text{ MeV}$. Constraints on the ALP matter coupling $C_{a\phi}$ is studied less compared to gauge boson coupling, however several processes involving flavors have been studied to put bound on it [43]. The constraints on ALP-fermion coupling $C_{a\Phi}$ depends on the ALP mass. The higher mass range is tested through the rare meson decays. Rare meson decay at Beam Dump experiments (CHARM) sets tight constraints on $C_{a\Phi}$ for mass range $1 \text{ MeV} \leq M_a \leq 3 \text{ GeV}$ as $C_{a\Phi}/f_a < (3.4 \times 10^{-8} - 2.9 \times 10^{-6}) \text{ GeV}^{-1}$ [67]. For our interested mass range we summaries the existing tightest constraints in Table. II.

Bound on Coupling	ALP Mass Range	Observables
$\frac{C_{\tilde{G}}}{f_a} \leq 10^{-4} \text{ GeV}^{-1}$	$M_a \leq 0.1 \text{ GeV}$	mono-jet 8 TeV@LHC
$\frac{C_{a\gamma}}{f_a} \leq 10^{-5} \text{ GeV}^{-1}$	$M_a \sim 1 \text{ MeV}$	Beam Dump
$\frac{C_{\tilde{W}}}{f_a} \sim 10^{-5} \text{ GeV}^{-1}$	$0.175 \text{ GeV} \leq M_a \leq 4.78 \text{ GeV}$	BABAR Exp.
$\frac{C_{a\Phi}}{f_a} \sim 10^{-8} - 10^{-6} \text{ GeV}^{-1}$	$1 \text{ MeV} < M_a < 3 \text{ GeV}$	Rare meson decay

TABLE II: Summary of existing constraint on ALP couplings.

¹ For very low masses, tighter constraint exists but we do not discuss them here as we are interested in mass range $M_a \sim \text{MeV-few GeV}$.

Benchmark: To start analyzing the model, we choose ALP mass $M_a = 10$ GeV. ALP-Gauge boson couplings $C_{\tilde{B}} = C_{\tilde{W}}$, since ALP is mostly constrained through $C_{a\gamma}, C_{\tilde{G}}$ and we also choose $\frac{C_{\tilde{G}}}{f_a}, \frac{C_{a\gamma}}{f_a}$ of the order of 10^{-4} GeV $^{-1}$ and ALP-fermion coupling $\frac{C_{a\Phi}}{f_a} \sim 10^{-6}$ GeV $^{-1}$, which satisfy all of the above constraints.

ALP decay: ALP can decay into SM final states when kinematically accessible, such as leptons, gauge bosons (W^\pm, Z, γ, g) and hadrons. Analytical form of these decay widths are listed in Appendix A. We found that for the range of couplings considered by us, ALP decay width is small enough to use the narrow width approximation. In Fig. 1, we

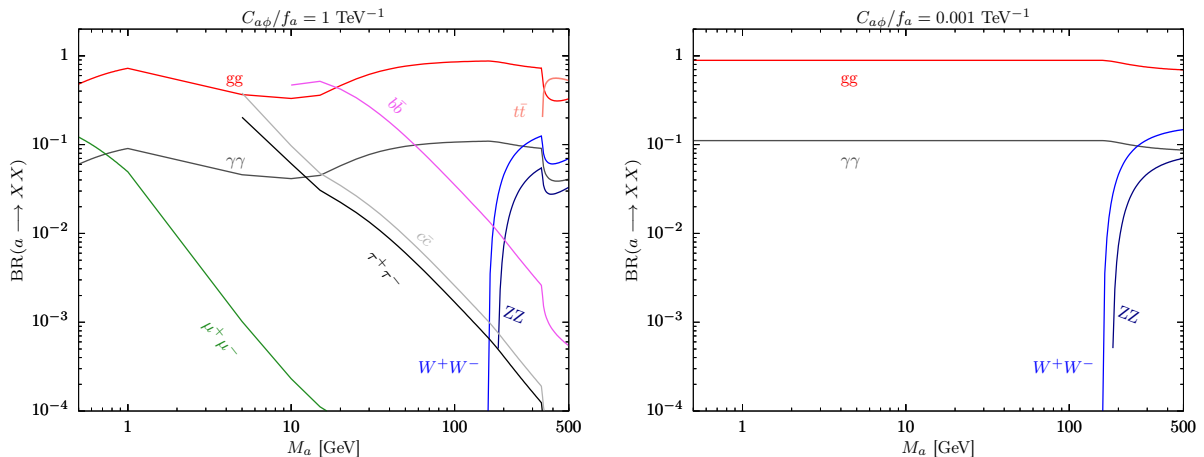


FIG. 1: The left and right panels show the variations of branching ratios for various decay channels with respect to ALP mass M_a . Different colors stand for different final states. In the right panel we choose smaller value of $C_{a\Phi}/f_a = 10^{-3}$ TeV $^{-1}$ to show that ALP decays dominantly to gauge bosons.

show the various branching ratios of ALP decay to SM final states. For left and right panel, we choose $C_{\tilde{G}}/f_a = C_{a\gamma}/f_a = 0.1$ TeV $^{-1}$, $C_{a\Phi}/f_a = 1$ TeV $^{-1}$ and $C_{\tilde{G}}/f_a = C_{a\gamma}/f_a = 0.1$ TeV $^{-1}$, $C_{a\Phi}/f_a = 0.001$ TeV $^{-1}$, respectively. We see from Fig. 1 that ALP mostly decays to gluon and photon pair. Also W^+W^- , ZZ pair contributes significantly as ALP mass crosses respective threshold values. Comparing the left panel with right panel one sees that lepton channels only contributes when $C_{a\Phi}$ is relatively large.

4. DARK MATTER ANALYSIS

So far we have discussed the constraints on ALP couplings to SM field. In this section we collect the results of our analyses of DM phenomenology. In our case N_1 plays the role of DM due to \mathbb{Z}_2 symmetry protection. In order to calculate all the vertices, the model is implemented in the FeynRules package [68]. All DM observables such as the thermal component of the DM relic abundance are determined using micrOMEGAS [69] which relies on CalcHEP [70] model file obtained from FeynRules. In the scanning of the relevant

parameters of the model, we have imposed phenomenological bounds we discussed earlier. The mass of $N_{2,3}$ is always chosen to be greater than N_1 for further analysis.

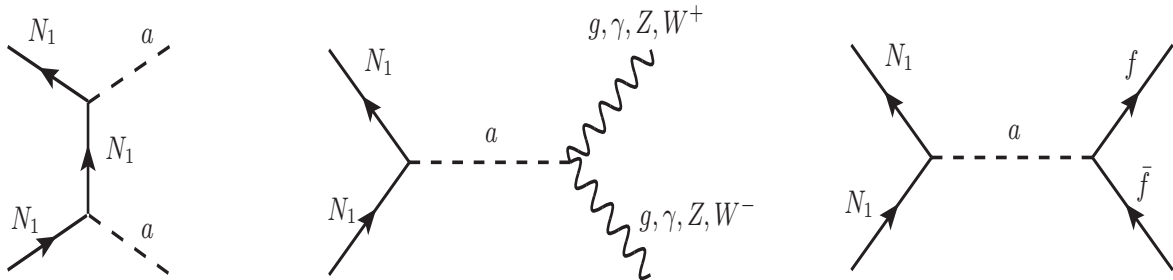


FIG. 2: Annihilation diagrams contributing to the relic abundance of N_1 .

4.1. Relic density

The relevant processes responsible for the freeze-out of DM in the early universe are shown in Fig. 2. All together, they determine the relic abundance of our assumed DM, N_1 . The annihilation cross section (σ) and thermal average annihilation cross section $\langle\sigma v\rangle$ and thus the relic abundance, scales straightforwardly with the parameters of the model. The exact analytical expressions for all the annihilation cross section are given in Appendix. B and Appendix. C. For our considered benchmark, only gauge bosons channels are relevant. We see that annihilation cross section for the process $N_1 N_1 \rightarrow f \bar{f}$ is negligible due to very small value of $C_{a\Phi}$. On the other hand with the limit $M_{N_1} > M_a$, $N_1 N_1 \rightarrow aa$ annihilation channel opens up but is v^2 suppressed. In Fig. 3, we show the annihilation

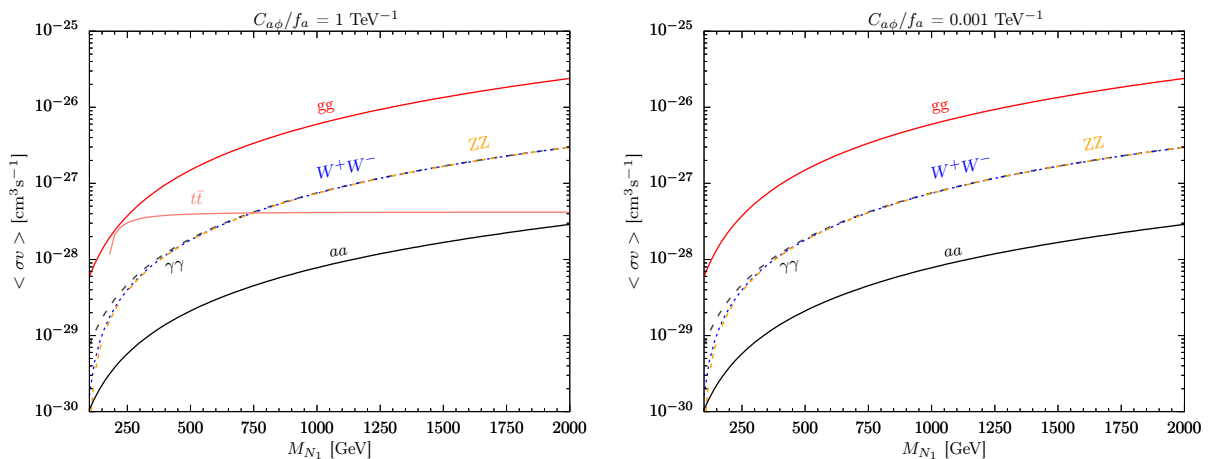


FIG. 3: Annihilation cross sections for different channels as a function of DM mass M_{N_1} . In the right panel we choose smaller value of $C_{a\Phi}/f_a = 10^{-3} \text{ TeV}^{-1}$ to illustrate that annihilation to gauge bosons dominate. In both panel we fix $C_{aN_1} = 0.1 \text{ TeV}^{-1}$.

cross section for different channels as a function of DM mass M_{N_1} . For left and right panel, we choose $C_{a\Phi}/f_a = 1 \text{ TeV}^{-1}$ and $C_{a\Phi}/f_a = 0.001 \text{ TeV}^{-1}$ respectively. For both panel we fix $C_{\tilde{G}}/f_a = C_{a\gamma}/f_a = C_{aN_1} = 0.1 \text{ TeV}^{-1}$. For relatively small value of $C_{a\Phi}/f_a$ annihilation cross section to gauge boson dominates over fermionic channels.

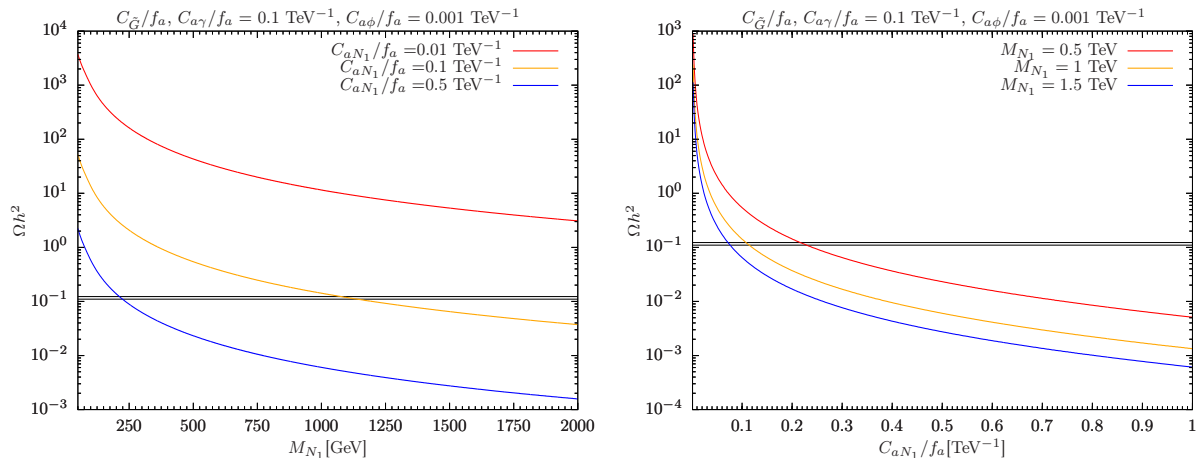


FIG. 4: The left panel shows the relic density ($\Omega_{N_1} h^2$) behavior with DM mass M_{N_1} for the chosen ALP parameters, labeled at the top. The three colored curves are due to three discrete choice of ALP- N_1 coupling. The region inside the horizontal black lines stands for the measured 3σ relic density range given by Planck satellite data, Eq. 6. The right panel is done using same analysis but with ALP- N_1 coupling varying continuously on the horizontal axis whereas mass of N_1 has been chosen discretely.

The left and right panel of Fig. 4 shows the relic density behaviour as a function of DM mass M_{N_1} and ALP-RHN coupling C_{aN_1} , respectively. In the left and right panel, three curves stand for three choices of ALP-RHN coupling and DM masses, respectively. The narrow horizontal band is the 3σ range for cold DM derived from the Planck satellite data [6]:

$$0.1126 \leq \Omega_{N_1} h^2 \leq 0.1246. \quad (6)$$

Only for solutions falling exactly within this band the totality of the DM can be explained by N_1 . We see from Fig. 4 that for smaller value of DM mass M_{N_1} , the required values of C_{aN_1}/f_a is relatively large to explain the correct relic density.

In Fig. 5 we show the region where the relic density bound $\Omega_{N_1} h^2 \leq 0.12$ holds on the $M_{N_1} - C_{aN_1}$ plane. In the left panel we have chosen three discrete values for the ALP-gluon coupling $C_{\tilde{G}}/f_a = 10^{-3} \text{ TeV}^{-1}$ (red), 10^{-2} TeV^{-1} (pink) and 10^{-1} TeV^{-1} (gray) by fixing other couplings as $C_{a\gamma}/f_a = 10^{-1} \text{ TeV}^{-1}$ and $C_{a\Phi}/f_a = 10^{-3} \text{ TeV}^{-1}$. In the right panel, the same analysis is done but now we have fixed $C_{\tilde{G}}/f_a = 10^{-1} \text{ TeV}^{-1}$ and choose three discrete values of ALP-photon coupling, $C_{a\gamma}/f_a = 10^{-3} \text{ TeV}^{-1}$ (red), 10^{-2} TeV^{-1} (pink) and 10^{-1} TeV^{-1} (gray). Note that in left (right) panel for relatively smaller values of ALP-

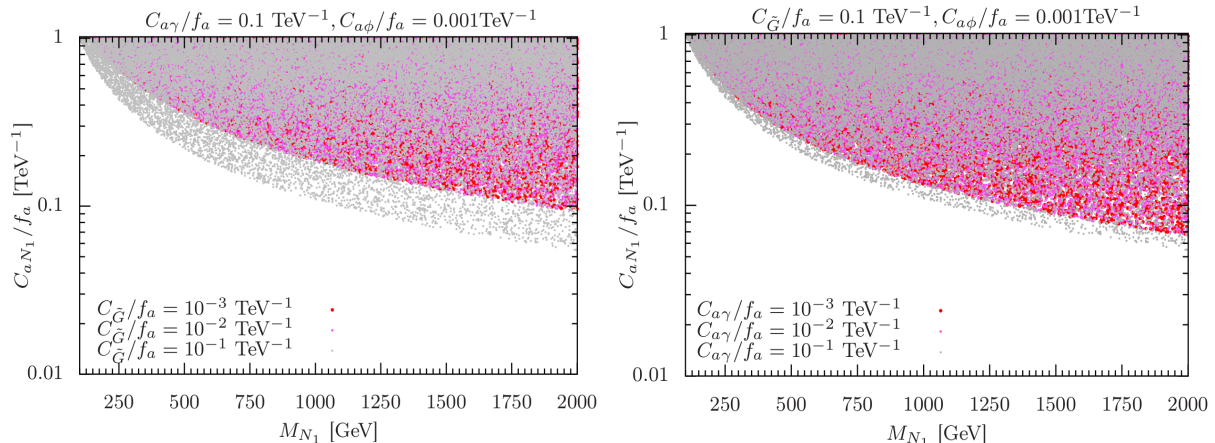


FIG. 5: The left panel describes the colored regions where the relic density bound ($\Omega_{N_1} h^2 \leq 0.12$) holds on the m_{N_1} - C_{aN_1} plane. We have chosen the three discrete values for the ALP-gluon coupling ($C_{\tilde{G}}$) labeled by the corresponding colors. In the right panel the same analysis is done but now with three discrete values for ALP-photon coupling ($C_{a\gamma}$).

gluon (ALP-photon) couplings red and pink region overlap. This happens due to subdominant contribution to the relic density of annihilation channel $N_1 N_1 \rightarrow gg$ ($N_1 N_1 \rightarrow \gamma\gamma$). We find that when gg channel dominates compared to other annihilation channel, the required value of C_{aN_1}/f_a is smaller to satisfy the relic density.

4.2. Direct detection

The XENON1T experiment [71] currently has the best sensitivity for spin-independent and spin-dependent DM-nucleon interactions in our interested mass range of DM. The interaction between DM N_1 and a quark q can be described by the following effective Lagrangian:

$$\mathcal{L} = \frac{C_{a\Phi} C_{aN_1}}{f_a^2 M_a^2} m_q M_{N_1} \bar{q} \gamma_5 q \bar{N}_1 \gamma_5 N_1. \quad (7)$$

Note that this is only valid when mediator ALP mass M_a is relatively large compared to momentum transferred involved in the scattering process. Following Ref. [43, 72–75] we found that in non-relativistic limit, differential scattering cross section to scatter of a nucleus is $d\sigma/dE_R \propto q^4$, where $q^2 = 2m_N E_R$ is the momentum transfer, m_N is the mass of nucleus and E_R is the nuclear recoil energy. In direct detection experiments typical recoil energy is $\mathcal{O}(10 \text{ KeV})$, hence direct detection cross section is heavily suppressed.

4.3. Indirect detection

If DM N_1 annihilates to SM final states with annihilation cross section near the thermal relic benchmark value $\langle\sigma v\rangle \sim 3 \times 10^{-26} \text{ cm}^3/s$, it may be detected indirectly. Perhaps, γ rays are the best messengers since they proceed almost unaffected during their propagation, thus carrying both spectral and spatial information. These γ -rays can be produced from DM annihilation, either mono-energetically from direct annihilation $N_1 N_1 \rightarrow \gamma\gamma$, γX or with continuum spectra from decays of the annihilation products $N_1 N_1 \rightarrow X \bar{X}$ ($X = \text{SM state}$).

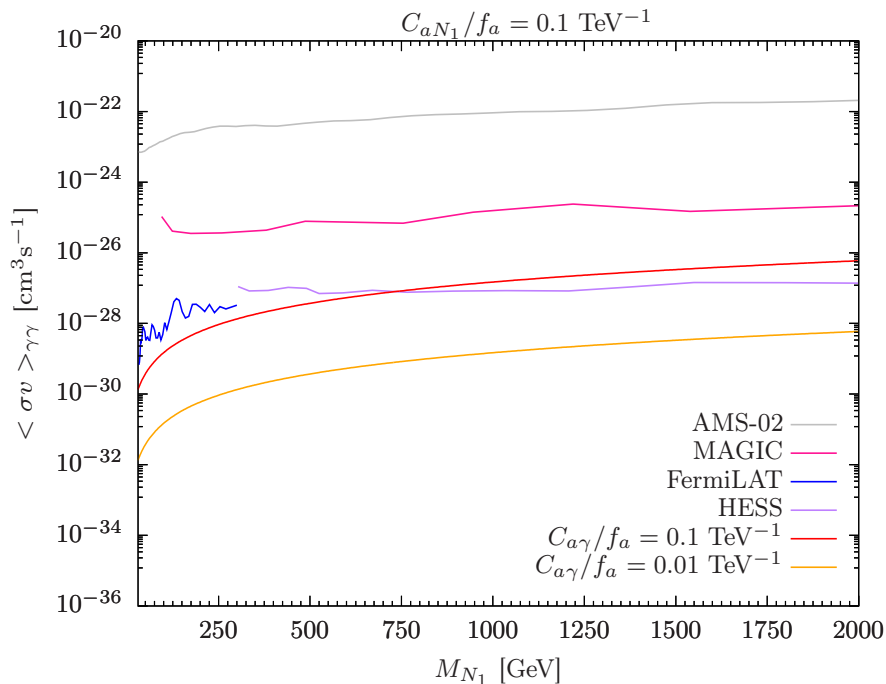


FIG. 6: Above plot shows the thermally averaged annihilation cross section for di photon emissions. Experimental limits obtained from AMS-02 (Grey) [77], MAGIC (Dark-Pink) [76], FermiLAT (Blue) [78], HESS (Purple) [76] data are shown. The red and orange lines are the model predictions for different choices of ALP-photon couplings $C_{a\gamma}/f_a$.

These γ rays would be produced preferentially in regions of high DM density and can be best detectable by Fermi-LAT [78], HESS [76]. The integrated γ -ray flux from the DM annihilation in a density distribution $\rho(\mathbf{r})$ is given by

$$\Phi_\gamma(\Delta\Omega) = \frac{1}{4\pi} \frac{\langle\sigma v\rangle}{2M_{N_1}^2} \int_{E_{\min}}^{E_{\max}} \frac{dN_\gamma}{dE_\gamma} dE_\gamma \cdot J, \quad (8)$$

where $J = \int_{\Delta\Omega} \int_{\text{l.o.s}} \rho^2(\mathbf{r}) d\ell d\Omega'$ is the line-of-sight (l.o.s) integral through the DM distribution integrated over a solid angle $\Delta\Omega$. The integral $\int^{\text{ROI}} \frac{dJ}{d\Omega} d\Omega$ represents the astrophysical component of the DM flux calculation in particular Region of Interest (ROI). AMS-02 look for excess positron flux in the positron energy range $\sim 1 \text{ GeV}$ to $\sim 500 \text{ GeV}$ over the cosmic

positron background. These positron can give rise two photon in final state after subsequent process. A model independent study of such bounds is studied[77]. FermiLAT collaboration look for direct DM annihilation to two photons from dwarf spheroidal galaxies of Milky Way in photon energy from few GeV to few hundreds of GeV. Higher energy range is being explored by MAGIC and HESS collaboration. We have considered the current upper limit from AMS-02, MAGIC, HESS, and annihilation data from FermiLAT respectively in Fig. 6 on thermally averaged annihilation cross section of di- γ final state along with our model predictions for our chosen benchmark in Fig. 6. The model prediction for ALP-photon coupling $C_{a\gamma}/f_a = 0.1 \text{ TeV}^{-1}$ lie very close to the Fermi-LAT and HESS upper limit. This suggests that future sensitivities of Fermi-LAT or HESS can either probe or exclude large parameter space of the model considered by us.

5. CONCLUSION

We have analyzed heavy neutrino DM candidate in a minimal extension of SM, which features three RHNs and one ALP. This model is well motivated as it not only accounts for DM, but it also explains the neutrino oscillations. Hence, ALP mediated RHN DM is interesting from both the model-building and phenomenological perspectives. We have considered the lightest RHN as DM which is odd under \mathbb{Z}_2 symmetry and identified the region of parameters where DM predictions are in agreement with DM relic abundance. In addition, this model also quite naturally explain the null results of LUX and XENON1T due to the pseudoscalar nature of interactions with quarks. We have highlighted the importance of complementary searches, for instance via indirect detection with single and di-photon. Although the current limits from Fermi-LAT lie above the predicted signals for our choice of parameter space, future sensitivities of Fermi-LAT might offer promising prospects to probe both the low as well as high DM mass regions.

ACKNOWLEDGMENTS

The work of SM is supported by the Spanish grant FPA2017-85216-P (AEI/FEDER, UE) and PROMETEO/2018/165 (Generalitat Valenciana).

Appendix A: ALP Decay Widths

$$\begin{aligned}
\Gamma_{agg} &= \frac{2C_{\tilde{G}}M_a^3}{\pi f_a^2}, \quad \Gamma_{a\gamma\gamma} = \frac{M_a^3(C_{\tilde{B}}\cos^2\theta_w + C_{\tilde{W}}\sin^2\theta_w)^2}{4\pi f_a^2}, \quad \Gamma_{aW^+W^-} = \frac{C_{\tilde{W}}^2(M_a^2 - 4M_W^2)^{\frac{3}{2}}}{2\pi f_a^2} \\
\Gamma_{a\gamma Z} &= \frac{\sin^2\theta_w \cos^2\theta_w (C_{\tilde{B}} - C_{\tilde{W}})^2 (M_a^2 - M_Z^2)^3}{2\pi f_a^2 M_a^3}, \quad \Gamma_{aff} = \frac{N_c C_{a\phi}^2 M_f^2 \sqrt{M_a^2 - 4M_q^2}}{8\pi f_a^2} \\
\Gamma_{aZZ} &= \frac{(C_{\tilde{W}}\cos^2\theta_w + C_{\tilde{B}}\sin^2\theta_w)^2 (M_a^2 - 4M_Z^2)^{\frac{3}{2}}}{4\pi f_a^2}, \quad \Gamma_{aN_i} = \frac{C_{aN_i}^2 m_{N_i}^2 \sqrt{M_a^2 - 4m_{N_i}^2}}{\pi f_a^2} \quad (A1)
\end{aligned}$$

where $N_c = 3(1)$ for quark(lepton).

Appendix B: Annihilation cross sections

$$\begin{aligned}
\sigma_{gg} &= \frac{16C_{aN_1}^2 C_{\tilde{G}}^2 M_{N_1}^2 s^2}{\pi f_a^4 (M_a^2 - s)^2 \sqrt{1 - \frac{4M_{N_1}^2}{s}}}, \quad \sigma_{\gamma\gamma} = \frac{2C_{aN_1}^2 [C_{\tilde{B}}\cos^2\theta_w + C_{\tilde{W}}\sin^2\theta_w]^2 M_{N_1}^2 s^2}{\pi f_a^4 (M_a^2 - s)^2 \sqrt{1 - \frac{4M_{N_1}^2}{s}}} \\
\sigma_{ZZ} &= \frac{2C_{aN_1}^2 [C_{\tilde{W}}\cos^2\theta_w + C_{\tilde{B}}\sin^2\theta_w]^2 M_{N_1}^2 s^2 (1 - \frac{4M_Z^2}{s})^{3/2}}{\pi f_a^4 (M_a^2 - s)^2 \sqrt{1 - \frac{4M_{N_1}^2}{s}}}, \\
\sigma_{W^+W^-} &= \frac{2C_{aN_1}^2 C_{\tilde{W}}^2 M_{N_1}^2 s^2 (1 - \frac{4M_W^2}{s})^{3/2}}{\pi f_a^4 (M_a^2 - s)^2 \sqrt{1 - \frac{4M_{N_1}^2}{s}}}, \quad \sigma_{ff} = \frac{N_c C_{aN_1}^2 C_{a\phi}^2 M_{N_1}^2 M_f^2 s \sqrt{1 - \frac{4M_f^2}{s}}}{2\pi f_a^4 (M_a^2 - s)^2 \sqrt{1 - \frac{4M_{N_1}^2}{s}}}, \\
\sigma_{aa} &= \frac{4C_{aN_1}^4 M_{N_1}^2}{\pi f_a^4 s} \sqrt{\frac{s - 4M_a^2}{s - 4M_{N_1}^2}} \left(2s - \frac{4M_a^4 M_{N_1}^2}{M_a^4 - 4M_a^2 M_{N_1}^2 + M_{N_1}^2 s} \right. \\
&\quad \left. + \frac{8M_{N_1}^2 (2M_a^4 - 4M_a^2 s + s^2) \tanh^{-1} \left(\frac{\sqrt{(s-4M_a^2)(s-4M_{N_1}^2)}}{-s+2M_a^2} \right)}{(s - 2M_a^2) \sqrt{(s - 4M_a^2)(s - 4M_{N_1}^2)}} \right) \quad (B1)
\end{aligned}$$

here θ_w is the weinberg angle.

Appendix C: Thermal average annihilation cross sections

$$\begin{aligned}
(\sigma v)_{gg} &\approx \frac{256C_{aN_1}^2 C_G^2 M_{N_1}^6}{\pi f_a^4 (M_a^2 - 4M_{N_1}^2)^2}, \quad (\sigma v)_{\gamma\gamma} \approx \frac{32C_{aN_1}^2 [C_{\tilde{B}} \cos^2 \theta_w + C_{\tilde{W}} \sin^2 \theta_w]^2 M_{N_1}^6}{\pi f_a^4 (M_a^2 - 4M_{N_1}^2)^2} \\
(\sigma v)_{ZZ} &\approx \frac{32C_{aN_1}^2 [C_{\tilde{B}} \sin^2 \theta_w + C_{\tilde{W}} \cos^2 \theta_w]^2 M_{N_1}^3 (M_{N_1}^2 - M_Z^2)^{3/2}}{\pi f_a^4 (M_a^2 - 4M_{N_1}^2)^2}, \\
(\sigma v)_{W+W^-} &\approx \frac{32C_{aN_1}^2 C_{\tilde{W}}^2 M_{N_1}^3 (M_{N_1}^2 - M_W^2)^{3/2}}{\pi f_a^4 (M_a^2 - 4M_{N_1}^2)^2}, \quad (\sigma v)_{f\bar{f}} \approx \frac{2N_c C_{aN_1}^2 C_{a\phi}^2 M_{N_1}^3 M_f^2 \sqrt{M_{N_1}^2 - M_f^2}}{\pi f_a^4 (M_a^2 - 4M_{N_1}^2)^2}, \\
(\sigma v)_{aa} &\approx \frac{8C_{aN_1}^4 M_{N_1} v^2 \sqrt{M_{N_1}^2 - M_a^2} (32M_{N_1}^8 - 64M_a^2 M_{N_1}^6 + 48M_a^4 M_{N_1}^4 - 16M_a^6 M_{N_1}^2 + 3M_a^8)}{3\pi f_a^4 (2M_{N_1}^2 - M_a^2)^4}
\end{aligned} \tag{C1}$$

-
- [1] M. Bartelmann and P. Schneider, “Weak gravitational lensing,” *Phys. Rept.* **340** (2001) 291–472, [arXiv:astro-ph/9912508](#).
- [2] D. Clowe, A. Gonzalez, and M. Markevitch, “Weak lensing mass reconstruction of the interacting cluster 1E0657-558: Direct evidence for the existence of dark matter,” *Astrophys. J.* **604** (2004) 596–603, [arXiv:astro-ph/0312273](#).
- [3] D. Harvey, R. Massey, T. Kitching, A. Taylor, and E. Tittley, “The non-gravitational interactions of dark matter in colliding galaxy clusters,” *Science* **347** (2015) 1462–1465, [arXiv:1503.07675 \[astro-ph.CO\]](#).
- [4] **WMAP** Collaboration, G. Hinshaw *et al.*, “Nine-Year Wilkinson Microwave Anisotropy Probe (WMAP) Observations: Cosmological Parameter Results,” *Astrophys. J. Suppl.* **208** (2013) 19, [arXiv:1212.5226 \[astro-ph.CO\]](#).
- [5] **Planck** Collaboration, P. A. R. Ade *et al.*, “Planck 2015 results. XIII. Cosmological parameters,” *Astron. Astrophys.* **594** (2016) A13, [arXiv:1502.01589 \[astro-ph.CO\]](#).
- [6] **Planck** Collaboration, N. Aghanim *et al.*, “Planck 2018 results. VI. Cosmological parameters,” *Astron. Astrophys.* **641** (2020) A6, [arXiv:1807.06209 \[astro-ph.CO\]](#).
- [7] M. Lattanzi and M. Gerbino, “Status of neutrino properties and future prospects - Cosmological and astrophysical constraints,” *Front. in Phys.* **5** (2018) 70, [arXiv:1712.07109 \[astro-ph.CO\]](#).
- [8] P. F. de Salas, D. V. Forero, S. Gariazzo, P. Martínez-Miravé, O. Mena, C. A. Ternes, M. Tórtola, and J. W. F. Valle, “2020 global reassessment of the neutrino oscillation picture,” *JHEP* **02** (2021) 071, [arXiv:2006.11237 \[hep-ph\]](#).

- [9] P. Minkowski, “ $\mu \rightarrow e\gamma$ at a Rate of One Out of 10^9 Muon Decays?,” *Phys. Lett. B* **67** (1977) 421–428.
- [10] J. Schechter and J. W. F. Valle, “Neutrino Masses in SU(2) x U(1) Theories,” *Phys. Rev. D* **22** (1980) 2227.
- [11] R. N. Mohapatra and G. Senjanovic, “Neutrino Mass and Spontaneous Parity Nonconservation,” *Phys. Rev. Lett.* **44** (1980) 912.
- [12] J. Schechter and J. W. F. Valle, “Neutrino Decay and Spontaneous Violation of Lepton Number,” *Phys. Rev. D* **25** (1982) 774.
- [13] I. Dorsner and P. Fileviez Perez, “Upper Bound on the Mass of the Type III Seesaw Triplet in an SU(5) Model,” *JHEP* **06** (2007) 029, [arXiv:hep-ph/0612216](https://arxiv.org/abs/hep-ph/0612216).
- [14] B. Bajc, M. Nemevsek, and G. Senjanovic, “Probing seesaw at LHC,” *Phys. Rev. D* **76** (2007) 055011, [arXiv:hep-ph/0703080](https://arxiv.org/abs/hep-ph/0703080).
- [15] A. de Gouvea, J. Jenkins, and N. Vasudevan, “Neutrino Phenomenology of Very Low-Energy Seesaws,” *Phys. Rev. D* **75** (2007) 013003, [arXiv:hep-ph/0608147](https://arxiv.org/abs/hep-ph/0608147).
- [16] A. de Gouvea, “GeV seesaw, accidentally small neutrino masses, and Higgs decays to neutrinos,” [arXiv:0706.1732](https://arxiv.org/abs/0706.1732) [hep-ph].
- [17] A. Abada and M. Lucente, “Looking for the minimal inverse seesaw realisation,” *Nucl. Phys. B* **885** (2014) 651–678, [arXiv:1401.1507](https://arxiv.org/abs/1401.1507) [hep-ph].
- [18] D. Borah and A. Dasgupta, “Common origin of neutrino mass, dark matter and dirac leptogenesis,” *Journal of Cosmology and Astroparticle Physics* **2016** no. 12, (Dec, 2016) 034–034. <https://doi.org/10.1088/1475-7516/2016/12/034>.
- [19] P. Das and M. K. Das, “Phenomenology of keV sterile neutrino in minimal extended seesaw,” *Int. J. Mod. Phys. A* **35** no. 22, (2020) 2050125, [arXiv:1908.08417](https://arxiv.org/abs/1908.08417) [hep-ph].
- [20] A. Merle, “keV sterile neutrino Dark Matter,” *PoS NOW2016* (2017) 082, [arXiv:1702.08430](https://arxiv.org/abs/1702.08430) [hep-ph].
- [21] M. Drewes *et al.*, “A White Paper on keV Sterile Neutrino Dark Matter,” *JCAP* **01** (2017) 025, [arXiv:1602.04816](https://arxiv.org/abs/1602.04816) [hep-ph].
- [22] A. Abada, G. Arcadi, and M. Lucente, “Dark Matter in the minimal Inverse Seesaw mechanism,” *JCAP* **10** (2014) 001, [arXiv:1406.6556](https://arxiv.org/abs/1406.6556) [hep-ph].
- [23] R. D. Peccei, “QCD, strong CP and axions,” *J. Korean Phys. Soc.* **29** (1996) S199–S208, [arXiv:hep-ph/9606475](https://arxiv.org/abs/hep-ph/9606475).
- [24] R. D. Peccei, “The Strong CP problem and axions,” *Lect. Notes Phys.* **741** (2008) 3–17, [arXiv:hep-ph/0607268](https://arxiv.org/abs/hep-ph/0607268).
- [25] J. E. Kim and G. Carosi, “Axions and the Strong CP Problem,” *Rev. Mod. Phys.* **82** (2010) 557–602, [arXiv:0807.3125](https://arxiv.org/abs/0807.3125) [hep-ph]. [Erratum: *Rev.Mod.Phys.* 91, 049902 (2019)].
- [26] A. Hook, “TASI Lectures on the Strong CP Problem and Axions,” *PoS TASI2018* (2019) 004, [arXiv:1812.02669](https://arxiv.org/abs/1812.02669) [hep-ph].

- [27] M. P. Lombardo and A. Trunin, “Topology and axions in QCD,” *Int. J. Mod. Phys. A* **35** no. 20, (2020) 2030010, [arXiv:2005.06547 \[hep-lat\]](#).
- [28] S. Weinberg, “A New Light Boson?,” *Phys. Rev. Lett.* **40** (1978) 223–226.
- [29] F. Wilczek, “Problem of Strong P and T Invariance in the Presence of Instantons,” *Phys. Rev. Lett.* **40** (1978) 279–282.
- [30] Z. G. Berezhiani and M. Y. Khlopov, “Cosmology of Spontaneously Broken Gauge Family Symmetry,” *Z. Phys. C* **49** (1991) 73–78.
- [31] J. E. Kim, “Weak Interaction Singlet and Strong CP Invariance,” *Phys. Rev. Lett.* **43** (1979) 103.
- [32] M. A. Shifman, A. I. Vainshtein, and V. I. Zakharov, “Can Confinement Ensure Natural CP Invariance of Strong Interactions?,” *Nucl. Phys. B* **166** (1980) 493–506.
- [33] M. Dine, W. Fischler, and M. Srednicki, “A Simple Solution to the Strong CP Problem with a Harmless Axion,” *Phys. Lett. B* **104** (1981) 199–202.
- [34] A. Hook, S. Kumar, Z. Liu, and R. Sundrum, “High Quality QCD Axion and the LHC,” *Phys. Rev. Lett.* **124** no. 22, (2020) 221801, [arXiv:1911.12364 \[hep-ph\]](#).
- [35] K. J. Kelly, S. Kumar, and Z. Liu, “Heavy Axion Opportunities at the DUNE Near Detector,” [arXiv:2011.05995 \[hep-ph\]](#).
- [36] H. Georgi, D. B. Kaplan, and L. Randall, “Manifesting the Invisible Axion at Low-energies,” *Phys. Lett. B* **169** (1986) 73–78.
- [37] I. Brivio, M. Gavela, L. Merlo, K. Mimasu, J. No, R. del Rey, and V. Sanz, “ALPs Effective Field Theory and Collider Signatures,” *Eur. Phys. J. C* **77** no. 8, (2017) 572, [arXiv:1701.05379 \[hep-ph\]](#).
- [38] A. Salvio, A. Strumia, and W. Xue, “Thermal axion production,” *JCAP* **01** (2014) 011, [arXiv:1310.6982 \[hep-ph\]](#).
- [39] Y. Hochberg, E. Kuflik, R. McGehee, H. Murayama, and K. Schutz, “Strongly interacting massive particles through the axion portal,” *Phys. Rev. D* **98** no. 11, (2018) 115031, [arXiv:1806.10139 \[hep-ph\]](#).
- [40] K. Mimasu and V. Sanz, “ALPs at Colliders,” *JHEP* **06** (2015) 173, [arXiv:1409.4792 \[hep-ph\]](#).
- [41] J. Jaeckel and M. Spannowsky, “Probing MeV to 90 GeV axion-like particles with LEP and LHC,” *Phys. Lett. B* **753** (2016) 482–487, [arXiv:1509.00476 \[hep-ph\]](#).
- [42] A. Alves, A. G. Dias, and K. Sinha, “Diphotons at the Z -pole in Models of the 750 GeV Resonance Decaying to Axion-Like Particles,” *JHEP* **08** (2016) 060, [arXiv:1606.06375 \[hep-ph\]](#).
- [43] M. J. Dolan, F. Kahlhoefer, C. McCabe, and K. Schmidt-Hoberg, “A taste of dark matter: Flavour constraints on pseudoscalar mediators,” *JHEP* **03** (2015) 171, [arXiv:1412.5174 \[hep-ph\]](#). [Erratum: *JHEP* 07, 103 (2015)].

- [44] E. Izaguirre, T. Lin, and B. Shuve, “Searching for Axionlike Particles in Flavor-Changing Neutral Current Processes,” *Phys. Rev. Lett.* **118** no. 11, (2017) 111802, [arXiv:1611.09355 \[hep-ph\]](#).
- [45] K. Choi, K. Kang, and J. E. Kim, “Effects of η' in low-energy axion physics,” *Physics Letters B* **181** no. 1, (1986) 145–149.
<https://www.sciencedirect.com/science/article/pii/0370269386912736>.
- [46] A. Salvio and S. Scollo, “Axion-Sterile-Neutrino Dark Matter,” [arXiv:2104.01334 \[hep-ph\]](#).
- [47] A. Salvio, “A Simple Motivated Completion of the Standard Model below the Planck Scale: Axions and Right-Handed Neutrinos,” *Phys. Lett. B* **743** (2015) 428–434, [arXiv:1501.03781 \[hep-ph\]](#).
- [48] A. Alves, A. G. Dias, and D. D. Lopes, “Probing alp-sterile neutrino couplings at the lhc,” [arXiv:1911.12394 \[hep-ph\]](#).
- [49] A. Atre, T. Han, S. Pascoli, and B. Zhang, “The Search for Heavy Majorana Neutrinos,” *JHEP* **05** (2009) 030, [arXiv:0901.3589 \[hep-ph\]](#).
- [50] **Particle Data Group** Collaboration, K. A. Olive *et al.*, “Review of Particle Physics,” *Chin. Phys. C* **38** (2014) 090001.
- [51] N. Vinyoles, A. Serenelli, F. L. Villante, S. Basu, J. Redondo, and J. Isern, “New axion and hidden photon constraints from a solar data global fit,” *JCAP* **10** (2015) 015, [arXiv:1501.01639 \[astro-ph.SR\]](#).
- [52] G. G. Raffelt, “Astrophysical axion bounds,” *Lect. Notes Phys.* **741** (2008) 51–71, [arXiv:hep-ph/0611350](#).
- [53] A. Friedland, M. Giannotti, and M. Wise, “Constraining the Axion-Photon Coupling with Massive Stars,” *Phys. Rev. Lett.* **110** no. 6, (2013) 061101, [arXiv:1210.1271 \[hep-ph\]](#).
- [54] A. Ayala, I. Domínguez, M. Giannotti, A. Mirizzi, and O. Straniero, “Revisiting the bound on axion-photon coupling from Globular Clusters,” *Phys. Rev. Lett.* **113** no. 19, (2014) 191302, [arXiv:1406.6053 \[astro-ph.SR\]](#).
- [55] **CMS** Collaboration, V. Khachatryan *et al.*, “Search for dark matter, extra dimensions, and unparticles in monojet events in proton–proton collisions at $\sqrt{s} = 8$ TeV,” *Eur. Phys. J. C* **75** no. 5, (2015) 235, [arXiv:1408.3583 \[hep-ex\]](#).
- [56] **ATLAS** Collaboration, G. Aad *et al.*, “Search for new phenomena in final states with an energetic jet and large missing transverse momentum in pp collisions at $\sqrt{s} = 8$ TeV with the ATLAS detector,” *Eur. Phys. J. C* **75** no. 7, (2015) 299, [arXiv:1502.01518 \[hep-ex\]](#).
[Erratum: *Eur.Phys.J.C* 75, 408 (2015)].
- [57] G. Krnjaic, “Probing Light Thermal Dark-Matter With a Higgs Portal Mediator,” *Phys. Rev. D* **94** no. 7, (2016) 073009, [arXiv:1512.04119 \[hep-ph\]](#).

- [58] J. D. Clarke, R. Foot, and R. R. Volkas, “Phenomenology of a very light scalar ($100 \text{ MeV} < m_h < 10 \text{ GeV}$) mixing with the SM Higgs,” *JHEP* **02** (2014) 123, [arXiv:1310.8042](#) [[hep-ph](#)].
- [59] **XENON100** Collaboration, E. Aprile *et al.*, “First Axion Results from the XENON100 Experiment,” *Phys. Rev. D* **90** no. 6, (2014) 062009, [arXiv:1404.1455](#) [[astro-ph.CO](#)]. [Erratum: *Phys.Rev.D* 95, 029904 (2017)].
- [60] N. Viaux, M. Catelan, P. B. Stetson, G. Raffelt, J. Redondo, A. A. R. Valcarce, and A. Weiss, “Neutrino and axion bounds from the globular cluster M5 (NGC 5904),” *Phys. Rev. Lett.* **111** (2013) 231301, [arXiv:1311.1669](#) [[astro-ph.SR](#)].
- [61] O. Rodríguez-Tzompantzi, “Conserved laws and dynamical structure of axions coupled to photons,” *Int. J. Mod. Phys. A* **36** no. 33, (2021) 2150259, [arXiv:2001.07101](#) [[hep-th](#)].
- [62] **CAST** Collaboration, V. Anastassopoulos *et al.*, “New CAST Limit on the Axion-Photon Interaction,” *Nature Phys.* **13** (2017) 584–590, [arXiv:1705.02290](#) [[hep-ex](#)].
- [63] M. Bauer, M. Heiles, M. Neubert, and A. Thamm, “Axion-Like Particles at Future Colliders,” *Eur. Phys. J. C* **79** no. 1, (2019) 74, [arXiv:1808.10323](#) [[hep-ph](#)].
- [64] N. Vinyoles, A. Serenelli, F. L. Villante, S. Basu, J. Redondo, and J. Isern, “New axion and hidden photon constraints from a solar data global fit,” *Journal of Cosmology and Astroparticle Physics* **2015** no. 10, (2015) 015.
- [65] **BaBar** Collaboration, J. P. Lees *et al.*, “Search for an Axionlike Particle in B Meson Decays,” *Phys. Rev. Lett.* **128** no. 13, (2022) 131802, [arXiv:2111.01800](#) [[hep-ex](#)].
- [66] **E787** Collaboration, S. Adler *et al.*, “Further search for the decay $K^+ \rightarrow \pi^+ \nu \text{ anti-}\nu$ in the momentum region $P < 195\text{-MeV}/c$,” *Phys. Rev. D* **70** (2004) 037102, [arXiv:hep-ex/0403034](#).
- [67] **CHARM** Collaboration, F. Bergsma *et al.*, “Search for Axion Like Particle Production in 400-GeV Proton - Copper Interactions,” *Phys. Lett. B* **157** (1985) 458–462.
- [68] A. Alloul, N. D. Christensen, C. Degrande, C. Duhr, and B. Fuks, “FeynRules 2.0 - A complete toolbox for tree-level phenomenology,” *Comput. Phys. Commun.* **185** (2014) 2250–2300, [arXiv:1310.1921](#) [[hep-ph](#)].
- [69] G. Bélanger, F. Boudjema, A. Goudelis, A. Pukhov, and B. Zaldivar, “micrOMEGAs5.0 : Freeze-in,” *Comput. Phys. Commun.* **231** (2018) 173–186, [arXiv:1801.03509](#) [[hep-ph](#)].
- [70] A. Belyaev, N. D. Christensen, and A. Pukhov, “CalcHEP 3.4 for collider physics within and beyond the Standard Model,” *Comput. Phys. Commun.* **184** (2013) 1729–1769, [arXiv:1207.6082](#) [[hep-ph](#)].
- [71] **XENON** Collaboration, E. Aprile *et al.*, “Dark Matter Search Results from a One Ton-Year Exposure of XENON1T,” *Phys. Rev. Lett.* **121** no. 11, (2018) 111302, [arXiv:1805.12562](#) [[astro-ph.CO](#)].

- [72] C. Boehm, M. J. Dolan, C. McCabe, M. Spannowsky, and C. J. Wallace, “Extended gamma-ray emission from Coy Dark Matter,” *JCAP* **05** (2014) 009, [arXiv:1401.6458 \[hep-ph\]](#).
- [73] M. Freytsis and Z. Ligeti, “On dark matter models with uniquely spin-dependent detection possibilities,” *Phys. Rev. D* **83** (2011) 115009, [arXiv:1012.5317 \[hep-ph\]](#).
- [74] H.-Y. Cheng and C.-W. Chiang, “Revisiting Scalar and Pseudoscalar Couplings with Nucleons,” *JHEP* **07** (2012) 009, [arXiv:1202.1292 \[hep-ph\]](#).
- [75] S. Banerjee, D. Barducci, G. Bélanger, B. Fuks, A. Goudelis, and B. Zaldivar, “Cornering pseudoscalar-mediated dark matter with the LHC and cosmology,” *JHEP* **07** (2017) 080, [arXiv:1705.02327 \[hep-ph\]](#).
- [76] **HESS** Collaboration, H. Abdallah *et al.*, “Search for γ -Ray Line Signals from Dark Matter Annihilations in the Inner Galactic Halo from 10 Years of Observations with H.E.S.S.,” *Phys. Rev. Lett.* **120** no. 20, (2018) 201101, [arXiv:1805.05741 \[astro-ph.HE\]](#).
- [77] G. Elor, N. L. Rodd, T. R. Slatyer, and W. Xue, “Model-Independent Indirect Detection Constraints on Hidden Sector Dark Matter,” *JCAP* **06** (2016) 024, [arXiv:1511.08787 \[hep-ph\]](#).
- [78] **Fermi-LAT** Collaboration, M. Ackermann *et al.*, “Search for Gamma-ray Spectral Lines with the Fermi Large Area Telescope and Dark Matter Implications,” *Phys. Rev. D* **88** (2013) 082002, [arXiv:1305.5597 \[astro-ph.HE\]](#).